 STAT

Approved For Release 2009/08/26 : CIA-RDP88-00904R000100110

Third United Nations
International Conference
on the Peaceful Uses
of Atomic Energy

A/CONF.28/P/362a
USSR
May 1964
Original: RUSSIAN

Confidential until official release during Conference

# STUDY OF BERYLLIUM AND BERYLLIA AS NEUTRON MODERATORS

I.F.Zhezherun, A.K.Krasin, G.I.Plindov, I.P.Sadikov, V.A.Tarabanko, A.A.Chernyshev

## Introduction

Beryllium and beryllia are of interest in the nuclear engineering as construction materials of reactors of various types due to their good moderative properties, weak thermal neutron absorption and fast neutron multiplication in the reaction $Be^9(n,2n)$. Physical properties of beryllium and beryllia determining diffusion, moderation, scattering and multiplication of neutrons have been studied for a few years in the Kurchatov Institute of Atomic Energy (IAE). The main results are briefly presented in the report.

In addition, the fast neutron multiplication data obtained from the analysis of the critical assemblies in the Institute of Energetics of Academy of Science BSSR are presented.

## A. STUDY OF BERYLLIUM AND BERYLLIA AS NEUTRON MODERATORS (1)

I.F.Zhezherun, I.P.Sadikov, V.A.Tarabanko, A.A.Chernyshev
(The Kurchatov Institute of Atomic Energy)

### 1. Effect of beryllia microstructure and temperature on thermal neutron scattering cross-section

The microcrystallyne structure can essentially influence on the moderative and scattering properties of beryllia due to the effect of size and orientation of crystal grains on the scattering cross-section $\sigma_s$ . It is known that with the increasing of the grain size $\sigma_s$ decreases due to the extinction effect; their advantageous orientation (texture) which can appear in pressing or pressing out of BeO articles can cause the anisotropy of $\sigma_s$ . To make clear how much these effects are to be taken into account when calculating the reactors of BeO moderator, the total cross-section $\sigma_t$ ( $\sigma_t \simeq \sigma_s$ for BeO) was measured with the chopper for four samples with various grain size (see Fig.I). Sample I consisted of the plates I.2x7x21 mm produced by pressing out, sample 2-of the rods 3x4x23 mm produced by pressing, sample 3 made of the discs 30 mm in diameter, 3 mm thick produced by pressing out and sample 4- of the discs 38 mm in diameter, 3 mm thick produced by cold pressing. The microstructure analysis of the samples, carried out by Yu.G.Digaltsev and V.I.Kushakov, showed the all samples are closed packed crystallite of irregular polyhedron form. The grain sizes are shown in Fig.1, the mean size was determined as a square root of an average area of a grain in a microsection photograph. In different measurements the sample thickness varied between 3.2 g/cm$^2$ and 5.6 g/cm$^2$.

Under given experimental conditions the energy resolution was between 4 and 10% in the range 0.03-0.1 ev. To observe the anosotropy of $\sigma_t$ two series of measurements have been done with samples I and 2, the neutron beam being fallen both in parallel and normally to the directions of pressing or pressing out (Fig.2).

It is seen from these figures that at small energy (0.005-0.2 ev) the difference in $\sigma_t$ is 40% for the samples with the grain sizes 8$\mu$ and 29$\mu$ ; it may cause 10% change of the average spectrum scattering length $\lambda_s$ or the square diffusion length $L^2$ (see Table 1). The extinction effect does not practically influence on $\sigma_t$ if the grain size $\leq 10\mu$.

The presence of texture in the hexagonal BeO lattice seems to be observed in the best way from neutron wave reflection on the planes being normal or parallel to the c-axis of the crys-

tal elementary cell, i.e. from the reflections in which the first two indexes or the last one are equal to zero. The anisotropy of $\sigma_t$ is observed from the reflection on the plane (110) at E = 0.012 ev (see inserts on Fig.2) as reaching 25% of the partial or 7% of the measured cross-sections. The values of the cross-sections $\sigma_{\perp}^{110}$ and $\sigma_{\parallel}^{110}$ show the advantageous orientation of the crystal grains by c-axis of the elementary cell in direction of pressing out and normally to the pressing direction, if the neutron beam is normal or parallel to the pressing out or pressing directions. For other reflections the difference in $\sigma_{\perp}$ and $\sigma_{\parallel}$, if it is, does not exceed the measurement errors. Thus, the anisotropy of $\sigma_t$ is small and its influence on $L^2$ may be neglected.

In the range 1-10 ev where atom binding in the crystal lattice does not effect on scattering the measured value of $\sigma_t$ is constant and equals 10±0.15 barn for all the samples.

The temperature dependence of $\sigma_t$ is of importance for the calculation of the temperature reactivity coefficient. In Fig.3 the measurement results of $\sigma_t$ are shown for the sample of advantageous grain sizes 10–20 $\mu$ at T = 290; 800; 1300; 1500°K. In Fig.4 the temperature dependence of $\sigma_t(E)$ for some energies is plotted as well as that of $\bar{\sigma}_t$ and $(\overline{\sigma_t^{-1}})^{-1}$ averaged over the Maxwellian spectrum (at the neutron temperature $T_H$ = T + 100°K) and obtained from Fig.3.

The measured results reveal that with the sample heating: 1) the position of Bragg maxima are shifted towards less energies in accordance with the temperature expansion; 2) the value of the maxima decreases; 3) the value of $\sigma_t$ increases, the greater it will be the less the neutron energy E is. At E > 0.15 ev $\sigma_t$, $\bar{\sigma}_t$ and $(\overline{\sigma_t^{-1}})^{-1}$ have a minimum near T'-1300°K which can be explained by the competition of two processes: decreasing of the coherent elastic scattering and increasing of the coherent inelastic one with the temperature increase. Since oxygen and beryllium in BeO are anisotropic and the incoherent scattering in Be depending on the spin is small, the measured $\sigma_t$ can be practically divided only in two terms: the elastic and inelastic coherent scattering cross-section, $\sigma_t$ is mainly due to the latter at E < 0.0035 ev.

The change of $\sigma_t$ with the temperature in the range 290–1500°K can lead to the decreasing of $L^2$ by about 20%.

The sample density was 2.80–2.85 g/cm$^3$, i.e. it was less than the theoretical value 3.04 g/cm$^3$. Therefore the question appeared whether the scattering in small angles, caused by the refraction and the diffraction of the neutron waves at the boundaries between substance and air in the sample pores, effects on the measured $\sigma_t$. The additional measurements on BeO sample in the form of the fine-grained dust showed that the scattering in small angles can be neglected.

## 2. Study of thermal neutron diffusion in beryllium and beryllia

The diffusion parameters of Be and BeO were studied by means of the pulse method with the linear accelerator of IAE. The method, as is known, is to measure the damping coefficient $\alpha$ of the neutron density in the moderator block with time and to analyse consequently the dependence of $\alpha$ upon the block geometry parameter $B^2$:

$$\alpha = \Sigma_c v + DB^2 - CB^4 \tag{I}$$

where $\Sigma_c v$ is the absorption velocity, D and C are the coefficients of diffusion and diffusion cooling respectively.

The coefficient $\alpha$ was measured for 30 beryllium blocks at $B^2$ = 0.005–0.11 cm$^{-2}$ and for 27 beryllia blocks at $B^2$ = 0.004–0.095 cm$^{-2}$ (see Fig.5). The average Be density in blocks was 1.79 g/cm$^3$, that of BeO – 2.79 g/cm$^3$. The measurements of $\alpha$ for such great number of blocks allowed to obtain the more accurate diffusion parameters (see Table II) than those in [2–8].

The all experimental values of the coefficient D for Be, including the ones in Table II, coincide within the measurement errors; for BeO the difference is considerably higher than the error. For the coefficient C the data are in agreement for BeO but as for Be there is



362a

no such agreement.

The study of the cause of the experimental data dispersion for D and C showed that it may be essentially connected with the possible difference of the crystal structure of the materials under investigation. Thus the estimated calculations of D and C for BeO using the above $\phi_t$ for the samples with the grain sizes $8\mu$ and $29\mu$ give the values of D within 10% and the values of C within 60%. The effect of the term with $B^6$ in Eq. I is negligible as it is seen from the additional analysis of measurements by means of the computer.

In [9] for the explanation of the dispersion of C it was indicated on the neutron trap effect which must result in dependence of $\alpha$ upon the measurement conditions for small blocks (the neutron source power, the background level etc.). Our attempts to detect this dependence for the Be block of 20 $cm^3$ when the source power changes 10 times and the background level does 3 times failed (Fig.6).

The value of C measured give some information on the neutron slowing-down near the thermal equilibrium indicating the decrease of the mean logarithmic energy loss $\xi$ in Be and BeO approximately 4-5 times.

## 3. Measurement of moderation length in Be up to 1.46 ev and 0.3 ev

The slowing-down density $q(r, E_\tau)$ was measured in the rectangular prism 80x90x145 cm. The $U^{235}$ converter, irradiated by the neutron beam of the reactor thermal column, served as a neutron source; the indium foils in cadmium filters were used as the neutron detectors at 1.46 ev; the small plutonium chamber in the filter with mixture of samarium and gadolinium oxides [10] was the detector at energy 0.3 ev. The measurement results are presented in Fig.7 (for In) and in Fig.8 (for Pu chamber).

The measurements by means of the Pu chamber were carried out in each point under the following conditions:

1) the chamber was surrounded by the filter of 0.125 $g/cm^2$ Sm and 0.04 $g/cm^2$ Gd ($N_{SmGd}$);

2) the chamber was surrounded by the filter of 0.125 $g/cm^2$ Sm, 0.04 $g/cm^2$ Gd and 0.35 $g/cm^2$ Cd ($N_{SmGdCd}$);

3) the chamber without filters (N).

The neutron flux of 0.3 ev was obtained as the difference of the first two measurements $\phi_{0.3} = N_{SmGd} - N_{SmGdCd}$, and the thermal neutron flux $\varphi_T = N - (1-T)^{-1} N_{SmGd}$, where T is the transmission of the resonance neutrons by the filter Sm+Gd. The inaccuracy of the value T, determined from the calculation, effects slightly on $\varphi_T$, since $N_{SmGd} \ll N$.

The curves for $\varphi_{0.3}$ and $\varphi_T$ (Fig.11) at distances $r > 60$ cm from the source are parallel. It implies that at such distances the density of the slowing-down neutrons of 0.3 ev is negligibly small in comparison with the density of neutrons of the same energy in the established Maxwellian spectrum. Using the ratio $\varphi_{0.3}/\varphi_T = (6.58 \pm 0.1) \cdot 10^{-3}$ at distances $r > 60$ cm one can obtain the slowing-down density $q_{0.3}$ from the total flux $\varphi_{0.3}$.

From Figs.7, 8 it is seen that at distances $r \leq 30$ cm from the source the slowing-down density is approximated by the expression $q(r) \sim e^{-r^2/4\tau}$ with $\tau = 80 \pm 2$ $cm^2$ at $E_\tau = 1.46$ ev and with $\tau = 91.5 \pm 2.5$ $cm^2$ at $E_\tau = 0.3$ ev. At $r > 30$ cm the expression $q(r) \sim r^{-2} e^{-r/\lambda}$ is valid with $\lambda = 7.27 \pm 0.10$ cm at $E_\tau = 1.46$ ev and 0.3 ev; this expression presents evidently the density of the first collisions. Over the whole region of measurements ($r \leq 90$ cm) the kernel of moderation is well approximated by the expression (Fig.9)

$$K(r, E_\tau) = \sum_{i=1}^{3} \frac{P_i(E_\tau)}{(4\pi\tau_i)^{3/2}} e^{-r^2/4\tau_i} \qquad (2)$$

where $\tau_1 = 68 cm^2$, $\tau_2 = 130 cm^2$, $\tau_3 = 265 cm^2$

$P_1 = 0.0666$, $P_2 = 0.307$, $P_3 = 0.027$ at $E_\tau = 1.46$ ev

$P_1 = 0.541$, $P_2 = 0.422$, $P_3 = 0.037$ at $E_\tau = 0.3$ ev.



362 a

The square of moderation length (1/6 of the mean square displacement at moderation) proved to be equal to $L_f^2$ (1.46 ev) = 92 ± 1.5cm$^2$, $L_f^2$ (0.3 ev) = 104.5±2.0cm$^2$. Their difference $L_f^2$(1.46 → 0.3ev) = 12.5±2.5 cm$^2$ exceeds the value calculated by 60% with the assumption that a neutron collides with free atoms. Thus, in the range 1.46–0.3 ev the atom bond in BeO lattice significantly effects on the neutron moderation. The value of $L_f^2$(1.46 ev) is in agreement with the data obtained [11,12] but it is more accurate. There are no data available for $L_f^2$ (0.3) in literature.

4. Study of Neutron Slowing-Down in Be and BeO

The slowing-down of neutrons ~ 2 Mev in Be and BeO was studied on the linear accelerator of the IAE by impulse method, measuring the transmission for indium, cadmium and samarium filters (In, Cd, Sm have strong resonances at 1.46 ev, 0.178 ev and 0.0976 ev, respectively) by a small $BF_3$-counter. In addition to $BF_3$-counter the detector of 0.3 ev neutrons was also used. The detectors were placed in moderator block (Be–60$^3$cm$^3$, BeO–70.80.75 cm$^3$) along the neutron beam axis of the accelerator.

The measurement results for the value of the inverse transmission $\Pi^{-1}(t)$ vs time, which lasted after a neutron impulse moment, are shown in Fig.10. In the same figure the detector counting rate of 0.3 ev neutrons is given too (Pu-chamber, shielded by Sm+Cd). In these measurements the channel width of the time analyzer was from 1μ sec to 10μ sec.

From the curves of Fig.10 the maxima are clearly seen. For convenience, $\Pi^{-1}(t)$ is normalized to unit. The time corresponding to these maxima is obviously a neutron slowing-down time up to a given energy, $t_s$, plus the time of flight from the point of the last collision up to the neutron absorption in detector $t_f(\lambda_s(v) + \frac{d}{2})/v$ where v is the neutron velocity, d is the mean detector dimension (taking into account the detector hole).

In Table III the values $t_s$ are given. The errors result from the uncertainty of the position of the maximum, the former is connected with the channel analyzer width and with the inaccuracy of the calculation of $t_f$. The comparison of these values with calculated ones, obtained for the neutron scattering by free atoms shows that the crystical binding in Be and BeO is of importance for the slowing-down already in 1.46–0.3 ev range.

Measuring with Pu-chamber (Fig.14) made possible to derive another important slowing-down characteristic-time-energy distribution of moderating neutrons of 0.3 ev and to compare it with the theoretical one [13]:

$$N(r,u,t) \quad \frac{\xi v}{\lambda_s} N_{cm}(r,u) N_o(u,t) \left[1+\varepsilon(r,u,t)\right], \qquad (3)$$

where

$$N_o(u,t) = \frac{\left(1 - \frac{v}{v_o}\right)^{2/\xi - 1}}{\xi} \; \frac{\left(\frac{vt}{\lambda_s}\right)^{2/\xi} e^{-\frac{vt}{\lambda_s}}}{\Gamma\left(1+\frac{2}{\xi}\right)}, \qquad (4)$$

$N_o(u,t)$ is Poisson probability of appearence of $2/\xi$ neutrons during a time t, if the neutron appearence at any moment is equally probable and equal to $\frac{v}{\lambda_s} dt$ ($u$ is lethargy, $v_o$ and $v$ are initial and final neutron velocities). The full and dotted lines in Fig.11 correspond to Poisson distribution (4) with $2/\xi$ = 12 for Be and 18 for BeO, respectively. The discrepancy of theory and experiment at large t is connected with the effect of slowly increasing factor $1+\varepsilon$ in formula (3).

From the fact that the dispersion of Poisson distribution equals the average value and using the relations $\left(\frac{v t_s}{\lambda_s}\right)_{Be} = \frac{2}{\xi_{Be}} = 12$ and $\left(\frac{v t_s}{\lambda_s}\right)_{BeO} = 2/\xi_{BeO} = 18$, the slowing down time $t_s$ up to the energy 0.3 ev can be obtained independently of its determination from the position of the maximum (see Table III). For this purpose the dispersion $\Delta t = \frac{\Delta v}{v} t_1 = \frac{1}{2} \frac{\Delta E}{E} t$, (2.9μ sec for Be and 4.3μ sec for BeO) which is connected with energy range of detector sensitivity [10], is to be substracted from $t_s$. As a result we get 17.3μ sec for Be and 28μ sec for BeO, and also $\xi_{Be}$ = .19 and $\xi_{BeO}$=0.12.

The neutron slowing-down below 0.1 ev was studied by the measurement of the transmission



362a

of boron filters of 0.012 g/cm$^2$ and 0,025 g/cm$^2$ with I/V-detector, the detectors and filters being placed outside the block (see Fig.12). Due to collimator I only those neutrons may be detected which were directed to a block surface at the angle > 80°. It simplified significantly the calculation of the filter transmission $\Pi(T)$ vs the neutron temperature T. It was used then for deriving the temperature of moderated neutrons at the moment t from the transmission values measured with the assumption of Maxwellian distribution (see Figs.13 and 14, where $T_e$ is the equilibrium temperature at $t \to \infty$). In the calculations of $\Pi(T)$ either theoretical results for $\sigma_{tr}$ (E) in Be and BeO [14] were used or the experimental data obtained in [15] for $\sigma_t$ in Be and our data for $\sigma_t$ in BeO with the grain size 8$\mu$. The full and dotted lines in Fig.15 a,b correspond to those two ways of calculation of $\Pi(T)$. It is seen from these figures that below 0.7-0.5 ev T(t) tends to To exponentially, the relaxation time $\gamma^{-1}$ being practically independent of neither the filter thickness nor the way of calculation $\Pi(T)$. Besides the data in Fig. 13 and 14 the values $\gamma^{-1}$ for beryllium blocks of 50$^3$ cm$^3$ and for beryllia blocks of 60$^3$cm$^3$ were measured. After correcting for finite block sizes, the thermalization time $t_{th}$ = 185$\pm$20$\mu$ sec for Be and $t_{th}$ = 204$\pm$20$\mu$ sec for BeO, as a result, was obtained.

The measurements of $t_s$ and $t_{th}$ performed, give the possibility for deriving the value $\xi$ and making the following conclusions. The neutron slowing-down to 1.46 ev in Be and BeO is due to collisions with free atoms and lasts less than 10$\mu$ sec. In the range 1.46-0.3 ev a crystal binding effect reduced $\xi$ to 0.193$\pm$0.02 in Be and to 0.109$\pm$0.012 in BeO; $t_s$ in this range is 1.5-2 more than $t_s$ to 1.46 ev. In the range 0.3 $\sim$ 0.5 ev, below which the spectrum approximating that of Maxwellian is established, $\xi_{Be}$ = 0.049$\pm$0.005 and $\xi_{BeO}$ = 0.047$\pm$0.005 and $t_s$ is 6-7 more than $t_s$ to 1.46 ev. At E $\xi$ (0.05-0.025 ev) the moderation is very slow, on an average, up to 185$\mu$ sec in Be and up to 204$\mu$ sec in BeO. The mean logarithmic energy loss in this range for the whole neutron spectrum is dependent on the energy and determined by the thermalization time:

$$\xi = \frac{\lambda_s}{t_{th} v_\varphi} \sqrt{\frac{E_\varphi}{E}} \frac{E - E_\varphi}{E}$$

where $E_\varphi$ and $v_\varphi$ are the equilibrium energy and velocity.

The energy-time distribution of neutrons in the range to $\sim$ E$\approx$0.05 ev can be obtained from formula (4) by substituting the given values $\xi$. The same values were used for calculation of the slowing-down area below 1.46 ev (see Table IV).

The value $L_f^2$ (0.3 ev) for BeO is in a food agreement with the direct measurement data (see §3).

## 5. Multiplication of Fission Neutrons in Be and BeO in Be$^9$ (n, 2n) Reaction

The moderators containing Be give an additional neutron multiplication in reactors connected with the difference of contributions of (n,2n) and (n, $\alpha$) reactions. As the calculation of the coefficient of this multiplication possessed a large uncertainity [17] we measured $K_{Be}$ for Be in spherical geometry experiment. The experiment consisted in measurement of integral neutron fission source power N (fission converter of $U^{235}$ on the reactor beam), being shielded by a spherical layer of beryllium or graphite of various thickness (graphite was necessary for excluding the variation of the sensitivity of the detector ("allwave" $BF_3$-counter) with neutron energy). The presence of a hole in a beryllium and graphite spheres for transmission of reactor neutron beam into converter caused the anisotropy of fission source and led to determining the source power N as a result of integrating the counting rate, measuring on a horisontal plane at different angles to the beam axis. For reducing this anisotropy and excluding the corrections for a finite distance from the source to the detector, the spheres investigated were surrounded by a spherical wood layer 14 cm thick.

In Fig.16 the measurement results are shown of $N_c$ and $N_{Be}$ vs the mean neutron energy loss $\overline{\Delta E}$ when neutrons passed the graphite and beryllium layers and also $K_{Be}=N_{Be}(\overline{\Delta E})/N_c(\overline{\Delta E})$ is

362a

given. The value $\Delta\overline{E}$ was calculated with the effect of neutron "entangling" in elastic and inelastic collisions with Be and C, and it contains some uncertainity which is however of no importance for $K_{Be}$ (see Fig.17). Curve 2 of Fig.17 gives the more probable run of $K_{Be}$ vs a layer thickness. At 12–15 g/cm$^2$ Be $K_{Be}$ obtains the maximum value $1.10 \pm 0.015$. Using this value, the multiplication coefficient of fission neutrons was calculated in BeO too. It was assumed that $\frac{K_{BeO}-1}{K_{Be}-1} = \frac{n_{BeO}}{n_{Be}}$ where $n_{Be}$ and $n_{BeO}$ are the fission neutron collision density with beryllium atoms at neutron slowing-down in Be and BeO below the threshold of $Be^9(n, 2n)$, $Be^9(n,\alpha)$ and $O^{16}(n,\alpha)$ reactions. This assumption is approximately true, as at $E > 4$ Mev $\sigma_{n,2n}$ is nearly constant, and at $E < 4$ Mev the collision densities in Be and BeO are similar. As a result, $\frac{n_{BeO}}{n_{Be}} = \frac{1.34}{1.62}$ was obtained. Hence $K_{BeO} = 1.08 \pm 0.023$.

## B. CONTRIBUTION OF FAST EFFECTS ON Be TO THE MULTIPLICATION COEFFISIENT OF BERYLLIUM ASSEMBLIES

A.K.Krasin, G.I.Plindov,
The Institute of Energetics of Academy of Sciences BSSR

It is of interest to take into account the effect of (n,2n) and (n,$\alpha$) reactions on Be on critical masses and sizes of physical beryllium assemblies and to separate the contribution of fast effect into the multiplication coefficient.

For this purpose 10-group constants for beryllium were obtained. The Be (n,2n) reaction has considered as inelastic scattering leading to an additional neutron. The cross-sections of (n,2n) and (n,$\alpha$) reactions were taken in from [18–22] and [23,25], respectively.

For verification of constants obtained the neutron age of fission spectrum and fast-neutron multiplication coefficient in infinite homogeneous beryllium medium were calculated. The evaluated neutron age $\tau = 79$ cm$^2$ and the value of fast neutron multiplication coefficient $K_{Be} = 1.087$ were obtained, which are in a good agreement with the data [26] and with theoretical estimations [27,28], respectively.

With these constants the multiplication coefficients, critical masses and critical dimensions of physical assemblies, described in [29], were calculated in multi-group diffusion approximation, taking into account the reactions Be (n,2n) and Be (n, $\alpha$) ("a"-case) and with no account of them ("b"-case). The contribution of the fast effect on Be was defined as a difference of the multiplication coefficients, calculated with the account of Be(n,2n) and Be (n, $\alpha$) reactions or without it.

The results of calculations are shown in Table V. It is seen from Table V that the value of the fast effect on 9–10% Be is somewhat less, than the value $12 \pm 4\%$ given earlier for the same assemblies [29], but is within the experimental errors. Since the fast effect on Be was calculated in multigroup theory, the value of the present work seems more preferable.

362a

## REFERENCES


1. И.Ф. Жежерун, И.П.Садиков, А.А.Чернышов. [illegible] энергия 13, 250 (1962); И.Ф.Жежерун, И.П.Садиков, В.А.Тарабанько, А.А.[illegible]ов. Атомная энергия 13, 258 (1962); И.Ф.Жежерун. Атомная энергия 14, 19[illegible] (1963); И.Ф.Жежерун, И.П.Садиков, В.А.Тарабанько, А.А.Чернышов. Атомная энергия 15, 485 (1963). И.Ф.Жежерун. Атомная энергия 15, 505 (1963); И.Ф.Жежерун. Атомная энергия 16, 2[illegible] (1964). И.Ф.Жежерун. Изучение процесса замедления нейтронов в бериллии и окиси бериллия импульсным методом. Не опубликовано. Основные результаты докладываются на Женевской конференции.
2. А.В.Антонов и др. В книге "Физические исследования" Москва, изд-во АН СССР, 1955, стр.158 (Доклады советск.делегации на международной конференции по мирному использованию атомной энергии. Женева, 1955).
3. E.Campbel, P.Stelson. ORNL, 2076 (1956).
4. T.Komoto, F.Kloverstrom. Trans.Amer.Nucl.Soc., 1, 94 (1958).
5. G.de Saussure and E.G.Silver. Nucl.Sci.Abstr., 13, 1059 (1959); Nucl.Sci. and Eng., 6, 195 (1959); Proc. of Symposium Vienna, 17-20 October, 1960, p.500.
6. S.D.B.Iyenger, G.S.Mani, R.Ramanna and N.Umakanth Proc.Ind.Acad.Sci., XLV, s A, 265 (1957).
7. L.S.Kothary, P.G.Khubchandany, React. Sci.and Technol., 15, 30 (1961).
8. K.W.Seeman, Nucl. Sci.Abstr., 15, 1407 (1962).
9. G. de Saussure. Nucl.Sci. and Eng., 12, 433 (1962).
10. И.Ф.Жежерун, И.П.Садиков, А.А.Чернышов "Приборы и техника эксперимента" № 3, 43 (1962).
11. F.Benoist et al. Доклад № 1192, представленный Францией на вторую международную конференцию по мирному использованию атомной энергии (Женева, 1958).
12. G.A.Joanon, A.J.Goodjohn and N.F.Winker. Nucl.Sci.and Eng., 13, 171 (1962).
13. И.Г.Дядькин, Е.П.Батолина, Атомная энергия, 10, 5 (1961).
14. К.Сингви, Л.Кохари. Труды второй международной конференции по мирному использованию атомной энергии. Женева, 1958 г. Избранные доклады иностранных ученых, т.2, стр.67[illegible]. Атомиздат, Москва, 1959.
15. Д.Х.Хьюдж, Р.Б.Шварц. Атлас нейтронных сечений. Издание второе. Атомиздат, Москва, 1959.
16. Д.Юз. Нейтронные исследования на ядерных котлах, стр.161. Изд.иностранной литературы, Москва, 1954.
17. H.Rief, Nucl. Sci.and Eng., 10, 83 (1961).
18. J.S.Marion, J.S.Levin and L.Cranberg Phys.Rev., 114,(1959) p.1584.
19. G.J.Fischer,Phys. Rev. 108, 99 (1957).
20. J.R.Beyster, R.L.Henkel, R.A.Nobles and J.M.Kister. Phys.Rev., 98, 1216 (1955).
21. Ю.Г.Зубов, Н.С.Лебедев, В.М.Мороз. Сборник "Нейтронная физика" Госатомиздат, М.,1961.
22. W.P.Ball, M. McGregov and R.Booth. Phys.Rev., 110, 1392 (1958).
23. P.H.Stelson and E.C.Campbell, Phys.Rev., 106, 1252 (1957).
24. M.E.Battat and F.L.Ribe. 89, 80 (1953).
25. R.Bose and T.W.Bonner. Nucl.Phys.,23, 122 (1961).
26. М.Шапиро. Материалы комиссии по атомной энергии США. Ядерные реакторы, т.I,М.,(1956) 20[illegible].
27. K.C.Xines and J.R.Pollard, Journ.of Nucl.Energy, Part A-B, 16, 7 (1962)
28. P.G.Aline, F.E.Novak and B.Wolfe. Nucl.Sci.and Eng., 7, № 4, Letters (1960).
29. А.К.Красин, Б.Г.Дубовский, М.Н.Лонцов, Ю.Ю.Глазков, Р.К.Гончаров, А.В.Камаев, Л.А.Гер[illegible]ва, В.В.Вавилов, Е.И.Инютин, А.П.Сенченков. Труды Международной конференции по использованию атомной энергии в мирных целях.П Женева (1958). Доклад № 2146.


362a



Approved For Release 2009/08/26 : CIA-RDP88-00904R000100110005-4

Table 1

Value of $\bar{\sigma}_t$ and $(\overline{\sigma_t^{-1}})^{-1}$ averaged over the Maxwellian spectrum at the neutron temperature $T_n$ = 390°K

| Sample | Grain sizes, $\mu$ advantageous | Grain sizes, $\mu$ average | $\bar{\sigma}_t$, barn | $(\overline{\sigma_t^{-1}})^{-1}$, barn |
|---|---|---|---|---|
| I | 10–15 | 8 | 9.97 | 9.13 |
| 2 | 40 | 29 | 9.44 | 8.31 |
| 3 | 10–20 | 13 | 9.56 | 8.53 |
| 4 | – | 14 | 9.70 | 8.76 |

Table II

Diffusion parameters of Be and BeO

| Parameters | units | In Be | In BeO |
|---|---|---|---|
| $\Sigma_c v$ | $sec^{-1}$ | 262±11 | 174±6 |
| D | $cm^2/sec$ | $(1.24\pm0.013)\cdot10^5$ | $(1.56\pm0.01)\cdot10^5$ |
| C | $cm^4/sec$ | $(3.68\pm0.20)\cdot10^5$ | $(4.12\pm0.27)\cdot10^5$ |
| L | cm | 21.8±1.0 | 29.9±1.0 |
| Transfer length, $\lambda_{tr}$ | cm | 1.50±0.016 | 1.88±0.020 |
| Diffusion time, e | msec | 3.82±0.017 | 5.75±0.020 |
| Absorption cross section $\sigma_c$ at 2200 m/sec | mbarn | 10.0±0.4 | 11.8± 0.4 |

Table III

Slowing-down time (in $\mu$ sec) of ~ 2 Mev neutrons to various energies

| Slowing-down energy, eV | In Be calculation $\xi_1$ = 0.209 | In Be experiment | In BeO calculation $\xi$ =0.176 | In BeO experiment |
|---|---|---|---|---|
| 1.46 (In) | 7.2 | 7.5±1 | 9.3 | 9.5±1 |
| 0.3 (Pu) | 15.7 | 17.5±1 | 19.2 | 26±2 |
| 0.178 (Cd) | 20.4 | 40±3 | 26.3 | 51±3 |
| 0.0976 (Sm) | 27.6 | 73±5 | 34.8 | 88±5 |

362

Table IV

Slowing-down time $t_f$ and area $L_f^2$ of neutrons up to 1.46 ev in Be and BeO

| Energy range | In Be | | In BeO | |
|---|---|---|---|---|
| | $t_f$, $\mu$ sec | $L_f^2$, $cm^2$ | $t_f$, $\mu$ sec | $L_f^2$, $cm^2$ |
| 2 MeV – 1.46 eV | 7.5±1 | 85.8±16 | 9.5±1 | 92±1.5 |
| 2 MeV – 0.3 eV | 17.5±1 | 91.5±2.4 | 27±2 | 103.4±1.9 |
| 2 MeV – 0.178 eV | 40±3 | 98.9±26 | 51±3 | 112.1±2.1 |
| 2 MeV – 0.13 eV | 56±4*) | 103.4±2.7 | 69±4*) | 117.7±2.4 |
| 2 MeV – 0.0976 eV | 73±5 | 107.5±2.9 | 83±5 | 122.5±2.9 |
| 2 MeV – (0.07–0.045)eV | 135 | – | 160 | – |
| (0.07–0.045) – 0.025 eV | 185±20 | – | 204±25 | – |

*) It is calculated using the obtained values of $\xi$ in the energy range 0.3 – 0.0976 ev.

Table V

Calculation results of $K_{eff}$, critical sizes, critical masses and fast effect on Be

| Assembly | | $K_{eff}$ | $R_{cal}$ cm | $R_{exp}$ cm | $M_{cal}$ kg | $M_{exp}$ kg | $K_{Be}$ |
|---|---|---|---|---|---|---|---|
| graphite in fuel element | 4a | 1.0301 | 37.9 | 40.4 | 4.8 | 5.46 | 0.1016 |
| | 4b | 0.9286 | 48.4 | | | | |
| | 5a | 1.0341 | 34.7 | 37.5 | 5.02 | 5.86 | 0.0997 |
| | 5b | 0.9344 | 44.6 | | | | |
| | 6a | 1.0241 | 34.3 | 36.5 | 6.10 | 6.66 | 0.0971 |
| | 6b | 0.9270 | 45.3 | | | | |
| water in fuel element | 4a | 1.0396 | 28.9 | 31.5 | 2.78 | 3.31 | 0.0949 |
| | 4b | 0.9447 | 36.5 | | | | |
| | 5a | 1.0431 | 25.8 | 28.4 | 2.79 | 3.36 | 0.0928 |
| | 5b | 0.9503 | 32.5 | | | | |
| | 6a | 1.0420 | 23.9 | 26.2 | 2.85 | 3.42 | 0.0912 |
| | 6b | 0.9508 | 30.0 | | | | |

362a

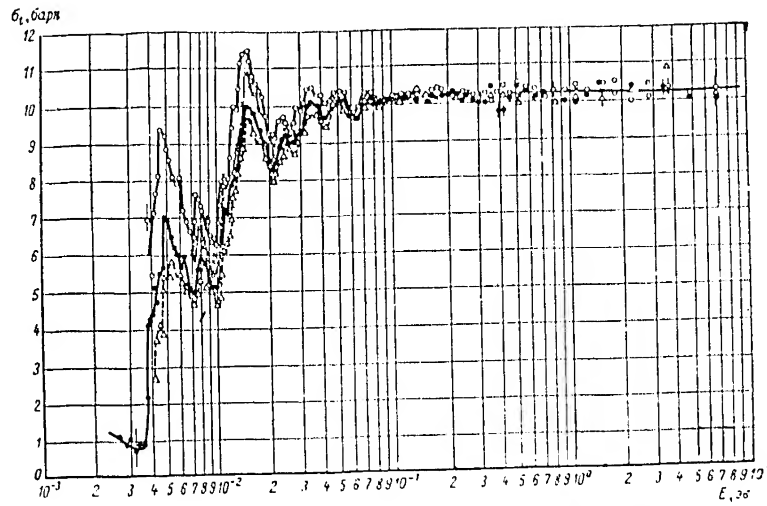


Fig.1. Total cross section $\sigma_t$ for the BeO samples of various crystal grain sizes; sample 1 (o): grain sizes = 4–23 $\mu$ , average size = 8 $\mu$ , advantageous sizes = 10–15 $\mu$ ; 2($\nabla$): sizes = 9–60 $\mu$, average one = 29 $\mu$ , advantageous one = 40 $\mu$ ; 3 (•): sizes = 5–37 $\mu$ , average one = 13 $\mu$ , advantageous ones = 10–20 $\mu$ ; 4 (x): sizes are large than ones of I and are less than ones of 3, average size = 14 $\mu$ .

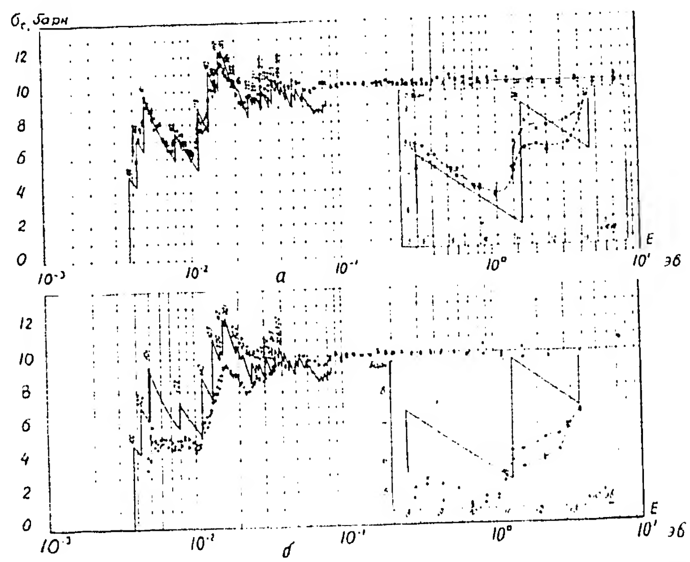


Fig.2. Total cross section for samples I and 2 produced by extrusion (a) and pressing (b). The incident neutron beam is parallel (•) and is normal to direction of extrusion and of pressing (x). The partial cross sections for the reflection from the plane (110) (see the insert) differ by 20–25%. The solid line represents the value of $\sigma_s$ calculated with the assumption of absence of the extinction and the account of only elastic scattering.

7620

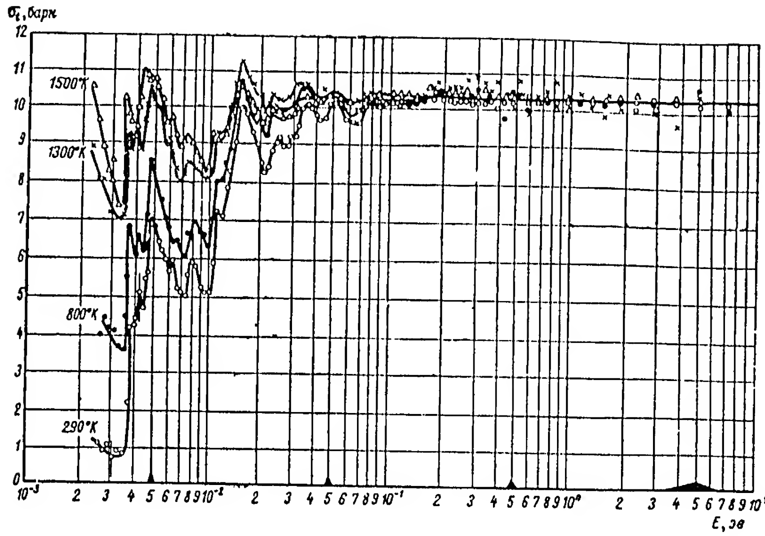


Fig.3. Total cross section $\sigma_t$ for BeO at various temperatures

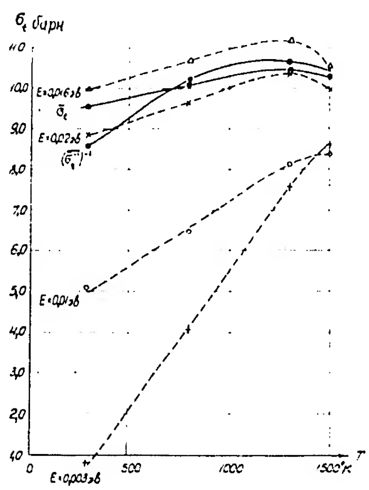


Fig.4. Total cross section for BeO vs temperature. $\bar{\sigma}_t$ and $(\overline{\sigma_t^{-1}})^{-1}$ are averaged over the Maxwellian spectrum for neutron temperature $T_n = T + 100°K$.

362a



Approved For Release 2009/08/26 : CIA-RDP88-00904R000100110005-4

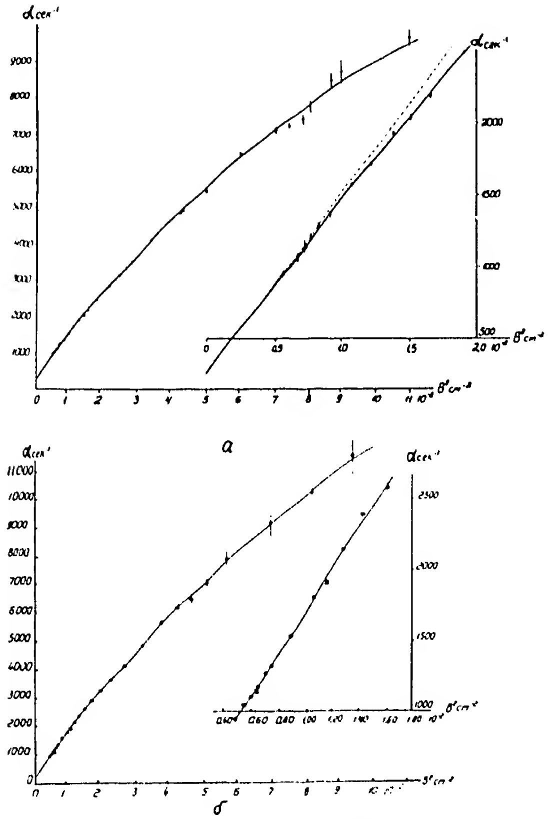

Fig.5. Damping coefficient $\alpha$ vs $B^2$ for Be (a) and BeO(b). The dots are the measurement results, the solid line corresponds to parabola (see Eq.(1) and Table II).

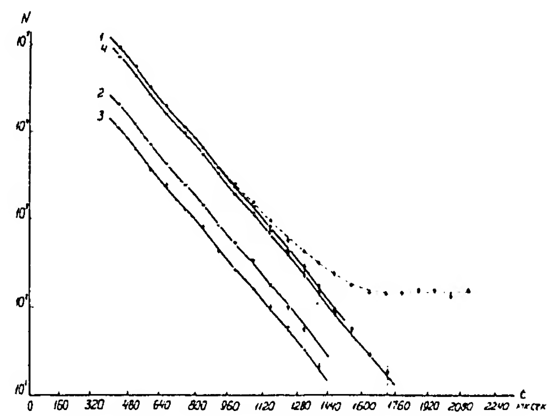

Fig.6. Neutron density damping in Be block of $20^3 cm^3$. 1,2,3 are various powers of a neutron source; 4-with the large background level. The dotted line represents the background plus the effect, the solid lines are obtained after the substraction of the background.

362 a

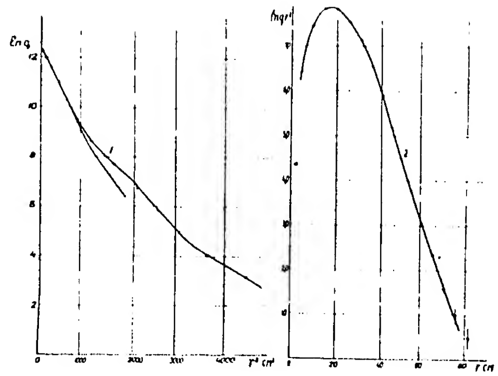

Fig.7. Moderation density at E = 1.46 eV for BeO in various coordinates

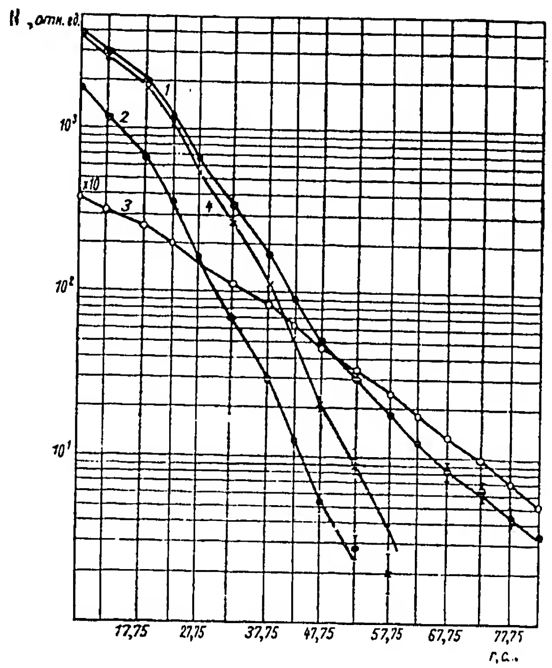


Fig.8. Measurement results with Pu-chamber: (1) flux of 0.3 ev neutrons $\Phi_{0,3}$ (2) contribution of higher resonances; (3) thermal neutron flux $\Phi_T$; (4) moderation density q at E = 0.3 ev. I - relative unit, II-g, cm

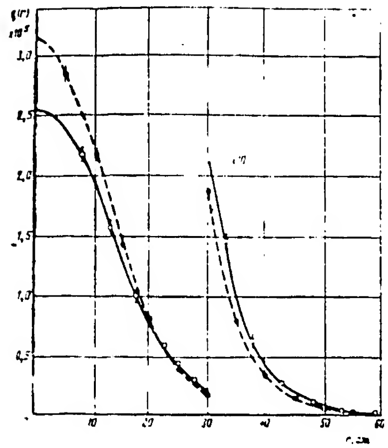

Fig.9. Comparison of the slowing-down densities at 0.3 ev(o) and 1.46 ev(•).The solid and dotted lines correspond the synthetic nuclei of type (2) at $E_r$=0.3 ev and 1.46 ev.

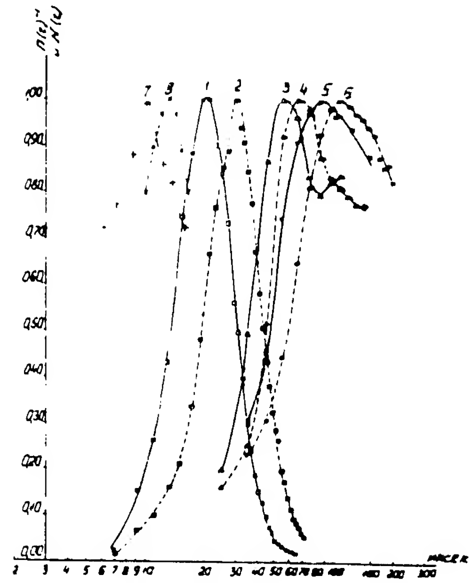

Fig.10. Measurement results of the slowing-down time. 1,2 are the detector counting rates N(t) of 0.3ev neutrons in blocks of Be and BeO, respectively; the inverse transmission $\Pi^{-1}(t)$ of Cd(3,4),Sm (5,6) and In(7,8) filters in Be and BeO.

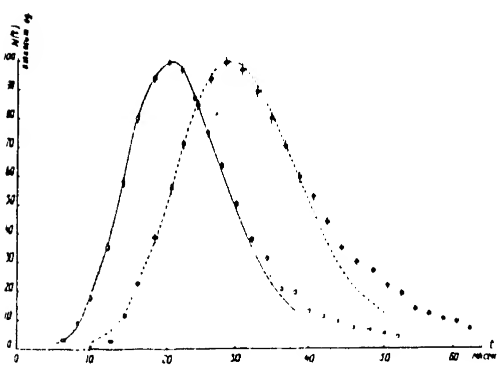

Fig.11. Experimental energy-time distribution of slowing-down neutrons at E =0.3 ev in comparison with the theoretical one. ○● -experiment for Be and BeO. The solid and dotted lines correspond to Poisson distribution: $N_{Be} \sim \left(\frac{vt}{\lambda_s}\right)^{12} e^{-\frac{vt}{\lambda_s}}$,

$$N_{BeO} \sim \left(\frac{vt}{\lambda_s}\right)^{18} e^{-vt/\lambda_s}$$

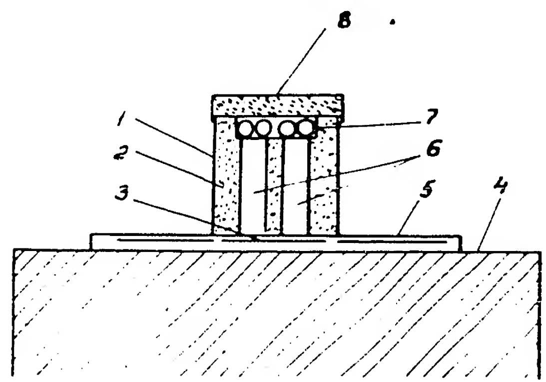


Fig.12.Experimental arrangement for studying of transmission through boron. 1-neutron collimator with Cd and $B_4C$; 2,3-filters; 4-moderator block; 5-collimator support; 6-collimator holes; 7-$BF_3$-counter; 8-shield of counters.



3626

Approved For Release 2009/08/26 : CIA-RDP88-00904R000100110005-4

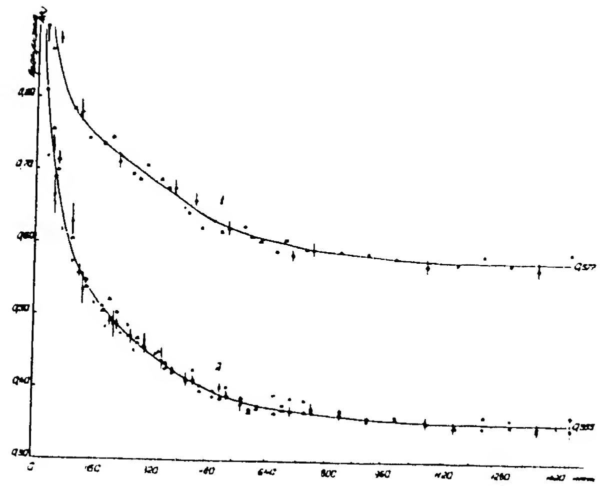

Fig.13. Transmission of boron filters for the Be block $60^3 cm^3$; I-filter 0.012 $g/cm^2$; 2-filter 0.023 $g/cm^2$; ϕ ϕ x ϕ -various measurement series.

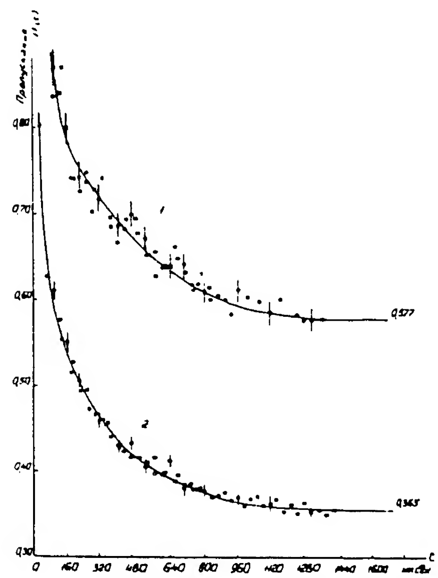

Fig.14.Transmission of boron filters for BeO block 70x80x75 $cm^3$. I-transmission; II-$\mu$ sec.

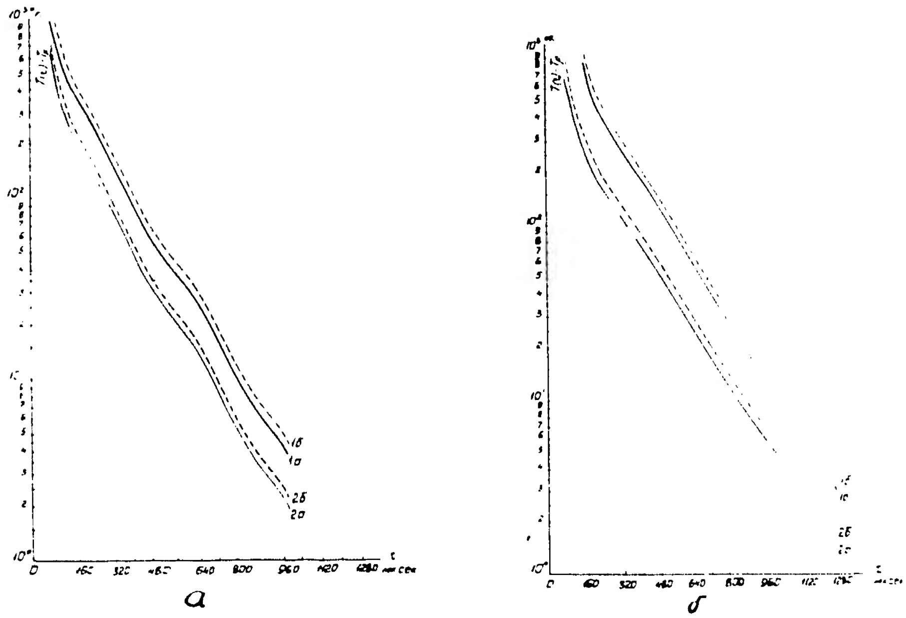

Fig.15. Neutron temperatures in Be(a) and BeO(b) vs slowing-down time (obtained from plats of Fig.13 and 14).

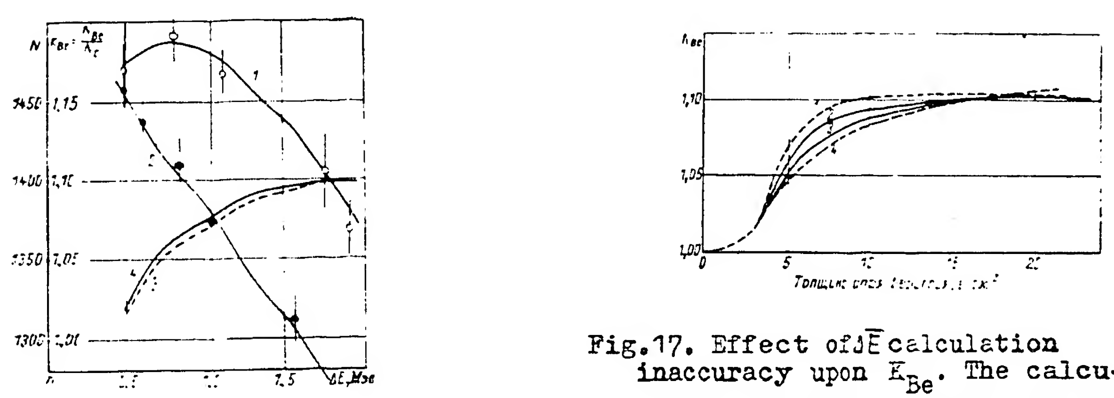

Fig.16. Integral counting rate N vs the average neutron energy loss $\Delta\bar{E}$: 1 - Be layer; 2 - graphite layer; 3 - $K_{Be}=N_{Be}(\Delta\bar{E})/N_c(\Delta\bar{E})$; 4 - $K_{Be}$ with correction of hole effect in spheres for the transmission of neutron beam

Fig.17. Effect of $\Delta\bar{E}$ calculation inaccuracy upon $K_{Be}$. The calculation variants: 1-with utilization of cross-sections on 15% as large in comparison with the data [15]; 2 - with utilization of cross-sections [15]; 3 - $K_{Be}$ with the account of neutron absorption in a wood sphere; 4 - with an assumption that $\sigma_{tr}=\sigma_s$. 1 - Beryllium layer thickness, g/cm$^2$